ELSEVIER

Tectonophysics 256 (1996) 253–277

TECTONOPHYSICS

Loading configurations and driving mechanisms for joints based on the Griffith energy-balance concept

Terry Engelder *, Mark P. Fischer [1]

The Department of Geosciences, The Pennsylvania State University, University Park, Pennsylvania 16802, USA

Received 25 October 1994; accepted 14 August 1995

Abstract

Using the Griffith energy-balance concept to model joint propagation in the brittle crust, two laboratory loading configurations serve as appropriate analogs for in situ conditions: the dead-weight load and the fixed-grips load. The distinction between these loading configurations is based largely on whether or not a loaded boundary moves as a joint grows. During displacement of a loaded boundary, the energy necessary for joint propagation comes from work by the dead weight (i.e., a remote stress). When the loaded boundary remains stationary, as if held by rigid grips, the energy for joint propagation develops upon release of elastic strain energy within the rock mass. These two generic loading configurations serve as models for four common natural loading configurations: a joint-normal load; a thermoelastic load; a fluid load; and an axial load. Each loading configuration triggers a different joint-driving mechanism, each of which is the release of energy through elastic strain and/or work. The four mechanisms for energy release are joint-normal stretching, elastic contraction, poroelastic contraction under either a constant fluid drive or fluid decompression, and axial shortening, respectively.

Geological circumstances favoring each of the joint-driving mechanisms are as follows. The release of work under joint-normal stretching occurs whenever layer-parallel extension keeps pace with slow or subcritical joint propagation. Under fixed grips, a substantial crack-normal tensile stress can accumulate by thermoelastic contraction until joint propagation is driven by the release of elastic strain energy. Within the Earth the rate of joint propagation dictates which of these two driving mechanisms operates, with faster propagation driven by release of strain energy. Like a dead-weight load acting to separate the joint walls, pore fluid exerts a traction on the interior of some joints. Joint propagation under fluid loading may be driven by a release of elastic strain energy and/or work by the pore fluid during poroelastic contraction. Again, propagation velocity dictates the driving mechanism, with critical to supercritical joint propagation accompanying fluid decompression and subcritical crack propagation taking place under a constant fluid drive. During axial shortening a jointing process called axial splitting may occur following wing crack growth from an initial crack tilted relative to the maximum compressive stress. Here the joint-driving mechanism may be either the work of a remote stress (i.e., a dead weight) or the release of elastic strain energy (i.e., fixed grips).

1. Introduction

The tensile strength of rock is best characterized by fracture toughness, a parameter that is independent of scale, specimen geometry, and loading con-

* Corresponding author

[1] Present address: Department of Geology, Northern Illinois University, DeKalb, IL 60115-2854, USA.

SSDI 0040-1951(95)00169-7

figuration. Common specimen geometries used during laboratory fracture toughness tests include the double-cantilever beam (Peck et al., 1985), the double-torsion plate (Meredith and Atkinson, 1983), the chevron-notched short rod (Barker, 1984), and the modified ring (Thiercelin and Roegiers, 1987). Each test geometry requires a slightly different loading device to grip and load the specimen. Despite the large variety of specimen shapes and loading devices there are two basic *loading configurations*: the dead-weight load and the fixed-grips load (Lawn and Wilshaw, 1975). Prior to crack growth, both loading configurations stretch or bend the test specimen elastically to open a preexisting crack (Fig. 1). Until failure by crack propagation, both loading configurations have the same effect on the test specimen.

Upon application of a dead-weight load, a specimen is stretched by a weight that is free to fall during crack propagation. In the laboratory, dead-weight loading is achieved by using a relatively compliant load frame. According to Griffith's (1920, 1924) analyses of crack propagation, energy for driving the crack under these conditions comes from the loss of potential energy by the falling weight or by relaxation of the load frame. In the fixed-grips loading configuration, a specimen is stretched a fixed amount and then held rigidly by grips (i.e., the loading device) that remain stationary during crack propagation. In this latter case, the loading device is restrained by a very stiff load frame. Here, energy for driving the crack comes from the release of elastic strain energy within the stretched or bent specimen. Of the two loading configurations, the dead-weight load is the more common laboratory configuration.

As is often the case, nature is more complex than the laboratory. There are at least four generic loading configurations in the Earth, all of which have laboratory analogs in the fixed-grips and dead-weight load experiments. Under each loading configuration joints are driven by a distinct type of energy release called a *joint-driving mechanism*. To explain the effect that each loading configuration has on joint propagation, we call upon the Griffith (1920, 1924) energy-balance criterion. Our purpose is to identify natural loading configurations during joint propagation in

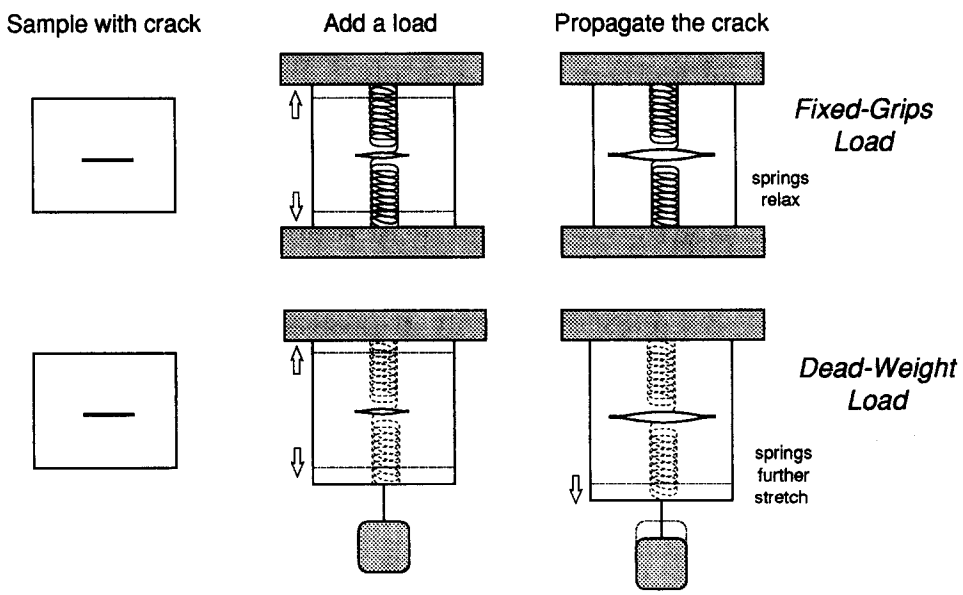

Fig. 1. Basic elements of fixed-grips and dead-weight loading configurations. The sample material is elastic (represented by springs). Prior to loading a small crack is placed within the elastic medium. Loading the sample has the effect of stretching the sample and opening the crack regardless of the loading configuration. In fixed-grips loading surface energy for crack propagation comes from the elastic relaxation of the elastic medium whereas in dead-weight loading the surface energy for crack propagation comes from the potential energy given up by the falling dead weight.

the Earth, and then to describe the joint-driving mechanism associated with each loading configuration. To prepare the reader for our analysis of joint-driving mechanisms, we start with a modest tutorial on the Griffith energy-balance concept. Then we discuss the various natural joint-driving mechanisms by giving field examples of each. Our major conclusion is that, contrary to the current notion that joint propagation in the Earth is analogous to a fixed-grips experiment, three of the four loading configurations have an element of energy release through dead-weight loading.

2. The Griffith energy-balance concept

2.1. Steam piston-cylinder

As an aid to understanding our model for each joint-driving mechanism we start with the workings of a steam piston-cylinder apparatus. The steam is characterized by an equation of state, the ideal gas law. If the steam is treated as a closed system of one component, the first law of thermodynamics states that the internal energy of the steam (U_{ST}) changes by the quantities of energy that enter or leave the system as heat (q) and work (w):

$$dU_{ST} = dq + dw \quad (1)$$

where dq is a quantity of heat supplied to the steam, and dw is the work done on the steam by the surroundings.

Now suppose that a steam piston-cylinder apparatus is a system with an internal component, steam, and an external component, a piston that carries a dead weight (Fig. 2). The moving piston is a loading device whose motion records a change in potential energy of the system. When expanding steam lifts the dead weight relative to its surroundings, the

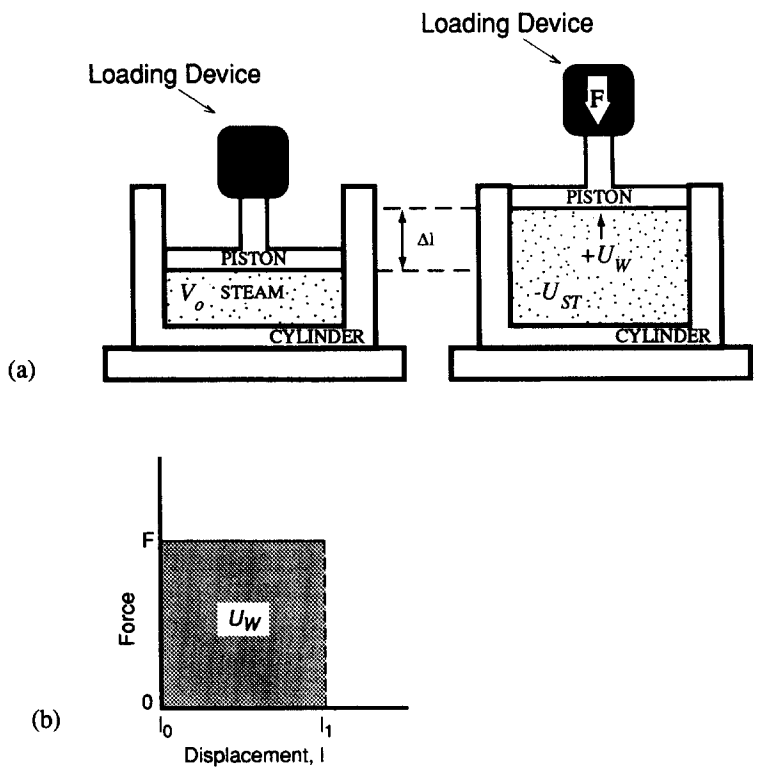

Fig. 2. The components of energy in a steam piston-cylinder system. (a) The steam piston-cylinder system has one internal component, steam, and one external component, the loading device. During an equilibrium expansion of the steam, energy is transferred from internal energy, U_{ST}, to potential energy, U_W, by lifting the loading device (i.e., the piston with dead weight). (b) Schematic force-displacement graph illustrating the increase in potential energy of the system (i.e., work done by lifting the dead weight).

steam piston-cylinder system is in a higher potential energy state, but the steam loses internal energy. By this action the steam does work (dU_W) on its surroundings (i.e., the piston) and a positive value is assigned for an increase in potential energy of the system. For an adiabatic equilibrium operation of the steam piston-cylinder system ($dq = 0$), the change in total energy of the system (dU_T), given by:

$$dU_T = dU_{ST} + dU_W \tag{2}$$

must be exactly zero for any increment, dl, of virtual piston motion (Fig. 2), such that:

$$\frac{dU_T}{dl} = 0 \tag{3}$$

Equilibrium is characterized by an exchange in energy between an internal component (U_{ST}) and an external component (U_W) without changing the total energy of the system. This formalized statement of energy balance in the steam piston-cylinder system is analogous to the Griffith energy balance for a rock-joint system as discussed below.

2.2. Equilibrium joint propagation

Griffith (1920, 1924) stated that equilibrium joint propagation requires the conservation of energy during propagation as expressed by:

$$\frac{dU_T}{dc} = 0 \tag{4}$$

where U_T is the total energy of a rock-joint system and dc is an increment of virtual joint extension. This is known as the Griffith energy-balance concept (Bueckner, 1958; Lawn and Wilshaw, 1975; Rice, 1978; Broek, 1987; Lawn, 1993).

A model for a rock with a joint subject to either a dead-weight or fixed-grips load is similar to a steam piston-cylinder apparatus (Fig. 3). Two differences are that the rock has two internal components rather than one and more than one possible loading config-

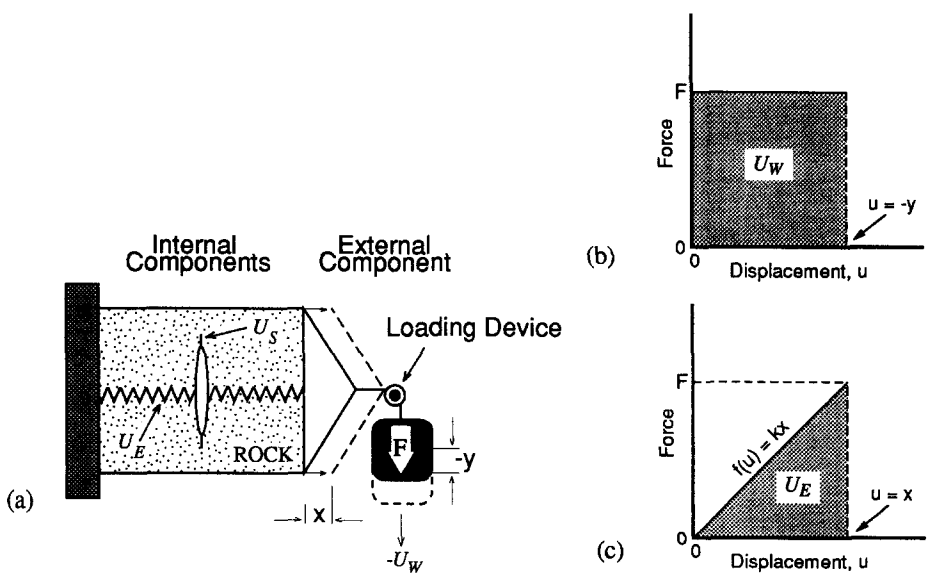

Fig. 3. Components of a rock-joint thermodynamic system. The internal components of the rock-joint system are the solid rock and the joint whereas the external component is the loading device. If the loading device acts on the crack wall as well as the external boundary of the rock, the cracked-rock system is said to have two external components. (a) Thermodynamic model for joint growth in rock (adapted from Pollard, 1989). As the joint grows, outer boundary of body moves outward by an amount x while the dead weight drops a distance of $-y$. The energy budget of the system includes surface energy (U_S), potential energy (U_W) and strain energy (U_E). (b) Schematic force-displacement graph illustrating the decrease in potential energy of the system (i.e., work done by the falling dead weight). (c) Schematic force-displacement graph illustrating the strain energy in the rock due to stretching.

uration. For a linear elastic rock-joint system, one internal component is the joint, defined in two dimensions by its length, $2c$, and aperture, $2b$. A second internal component is the solid rock, defined by elastic properties such as Young's modulus (E), and Poisson's ratio (ν). Each loading configuration is modeled as an external component of the rock-joint system.

Joint propagation consumes energy in the form of surface energy, U_S, for the newly created joint surface. The energy of the solid rock is specified as elastic strain energy, U_E (Fig. 3). As a joint propagates, the rock may undergo elastic strain and, hence, a change in elastic strain energy. In the rock-joint system, U_E and U_S characterize the internal energy of the system, and in combination are analogous to U_{ST} in the steam piston-cylinder system. To recast the equilibrium operation of a steam piston-cylinder system in terms of a rock-joint system, for equilibrium any change in the internal energy of the rock-joint system, $(U_S + U_E)$, must be balanced by a change in potential energy of the system (U_W), such that:

$$dU_S \pm dU_E = dU_W \tag{5}$$

This equation denotes the specific conditions required for conservation of energy during joint propagation as specified in Eq. (4).

In the rock-joint system there is the possibility for potential energy of the system to change through the action of more than one loading device. First, remote stress on a free-moving external boundary (i.e., a tectonic stress) is a load, analogous to the piston with a dead weight. A second dead-weight load may also arise from fluid pressure on the inside walls of a joint. If tectonic deformation moves the outer boundary of the rock-joint system, or if fluid within the joint moves the joint wall, work is done on the rock-joint system by a loading device. Motion of a boundary or joint wall represents a reduction in the potential energy of a loading device which energy is converted into work on the rock-joint system. Secor (1969) called these two work terms the potential of external forces and compressional fluid energy. Note that joint propagation does not require work from both loading devices simultaneously and, in some cases, does not require a contribution of work from either. When viewed from the system, the local rock-joint system does negative work (i.e., the loading device looses potential energy) on surrounding rock and any fluid acting within the joint. Hence, the potential energy term arising from the superposition of tractions from a remote stress and internal fluid pressure, is considered negative, in contrast to the steam piston-cylinder where dU_W is a positive quantity.

In the rock-joint system U_E and U_W are both forms of mechanical energy. Any change in potential energy of the loading device or elastic strain energy in the rock constitutes a change in mechanical energy (i.e., $-dU_W \pm dU_E$) of the system. Under adiabatic conditions (i.e., $dq = 0$) then, any change in the total energy, dU_T, of the system is given by the sum of changes in three terms:

$$dU_T = dU_S - dU_W \pm dU_E \tag{7}$$

During equilibrium joint propagation, the energy budget of the adiabatic rock-joint system is self adjusting as a consequence of the interaction of three energy sources or sinks: crack propagation, U_S, elastic deformation, U_E, and work of the dead weight, U_W. The Griffith energy-balance concept as represented by Eq. (4) therefore requires that the changes in the mechanical $(-dU_W \pm dU_E)$ and surface energy (dU_S) components of the rock-joint system must balance (i.e., $dU_S = (-dU_W \pm dU_E)$) over a virtual increment of joint extension dc. Because surface energy always increases during crack propagation, mechanical energy must decrease by at least the same amount to maintain equilibrium during joint propagation. Interestingly, equilibrium joint propagation can take place without a change in potential energy (U_W) of the rock-joint system if elastic strain energy (U_E) is exactly exchanged for surface energy (U_S). In fact, this is the energy exchange during joint propagation under fixed-grips loading. When delineating possible joint-driving mechanisms, one of the important factors concerns whether or not U_S consumes energy from the release of elastic strain energy or from work created by a change in the potential energy of a dead-weight load attached to the system. The answer to this question will in part determine the relative importance of fixed-grips and dead-weight loading configurations under geological conditions for in situ joint propagation.

2.3. Mechanical energy associated with joint propagation

The two components of mechanical energy in the Griffith energy-balance concept can be equated. If the loading device on the rock-joint system is attached to a dead weight, a change in potential energy of the dead weight upon stretching a jointed rock is measured as its weight, F, multiplied by the distance the weight moves, $-y$ (Fig. 3b):

$$U_W = \int_{u=0}^{u=-y} F\,du = -Fy \tag{8}$$

In contrast, any change in elastic strain energy, dU_E, within the rock is equivalent to the work of elastic loading (Fig. 3c):

$$U_E = \int_{u=0}^{u=x} f(u)\,du = \tfrac{1}{2}kx^2 = \tfrac{1}{2}Fx \tag{9}$$

where at $u=0$, $f(u)=0$ and at $u=x$, $f(u)=F$. Here $f(u)=kx$ is the functional relationship between force and displacement (e.g., Hooke's law). Because $f(u)$ is a constant in Eq. (8) and a linear function of displacement in Eq. (9), when $x=-y$, any change in the potential energy of a loading device attached to the boundary of a rock-joint system is twice the work of elastic loading on the system (compare Fig. 3b and 3c):

$$U_W = -2U_E \tag{10}$$

Fluid pressure within a joint also does work to drive joints, but during propagation the fluid pressure may decrease because the fluid is compressible. In this case the relationship between work of the fluid and the elastic strain energy is a more complex function of the compressibility of the fluid (Secor, 1969).

3. Geological considerations

3.1. Joint-driving stresses

The loading device on a steam piston-cylinder apparatus (i.e., the piston) has two analogs within the rock-joint system (Secor, 1969). One is the fluid within a joint that presses against the inside wall of the joint with a pressure, P_i. The other is the rock in which the immediate rock-joint system is encased. Before any joints have propagated $P_i = P_p$, where P_p is the pore pressure in the matrix of the rock. After the initiation of joint propagation $P_i \leq P_p$ (Engelder and Lacazette, 1990). Either loading device will elastically strain the rock-joint system upon the application of pressure and stress, respectively. Joint propagation is favored only when joint-normal stress is tensile (tension has a positive sign), a condition that either device is capable of producing. However, stress associated with burial (the least horizontal stress, S_h, in the case of vertical joints) may compress the rock-joint system and suppress any tendency for joint propagation. In this case, pore pressure, P_p, is required to overcome the compressive stress of burial and produce a state of effective tension (P_p has a positive sign). The joint will propagate when $(S_h + P_i) > 0$. $P_i + S_h$ is known as the *joint-driving stress* (Pollard and Segall, 1987).

In the analysis of joint propagation, the magnitude of the pore pressure and joint-normal stress and the shape and size of the joint are very important. As long as joint-driving stress is specified, we need know nothing more about the natural loading devices. As will be shown, there are three different joint-driving stresses: maximum horizontal stress $-S_H$, minimum horizontal stress S_h, and the internal pore pressure, P_i where $-S_H$ operates in the joint parallel direction and both S_h and P_i operate in the joint-normal direction.

The joint-parallel stress, $-S_H$, may contribute as a joint-driving stress for any joint tilted at a small angle to $-S_H$. The only way that $-S_H$ can drive a sharp-tipped crack is through shear stresses developed on a sliding crack tilted relative to $-S_H$ (Horii and Nemat-Nasser, 1985). In this situation a wing crack develops in the vicinity of the sharp tip and propagates by aligning with the $-S_H$ direction.

3.2. Initial energy of the rock-joint system

Although the energy-balance operates independently of the initial energy in the system, it is important to understand the initial energy of a system with a crack of length, $2c_o$, at some arbitrary depth of burial. The crack has an initial surface energy, U_s^i. An initial energy state is achieved during burial which is analogous to placing the dead weight

on the steam piston-cylinder with an initial volume, V_0 (Fig. 2). Deeply buried rock may be in a state of compression from overburden load or a state of tension from thermoelastic contraction.

Regardless of whether the rock is in tension or compression, the local rock-joint system will contain a total energy, U_T, proportional to the initial elastic strain energy, U_E^i, and the surface energy of any initial flaws or cracks in the rock:

$$U_T = \left(U_E^i\right)_{c=c_0} + \sum_{i=1}^{n} U_s^i = \frac{\left(-S_h\right)^2}{2E} + \sum_{i=1}^{n} U_s^i \quad (11)$$

where, for simplicity, $-S_h$ is the minimum horizontal compressive stress, E is the Young's modulus of the bulk rock and n is the number of initial flaws (Jaeger and Cook, 1969). We present Eq. (11) to illustrate the parameters that affect the initial energy of a rock-joint system, but note that one of the merits of the Griffith energy-balance concept is that equilibrium is specified in terms of the change of energy during joint propagation. Hence, it is not necessary to define the total energy terms which depend on some arbitrary initial state.

3.3. Propagation velocity of joints

Our interpretation of both loading configurations and joint-driving mechanisms is dependent on joint propagation velocity. Even though propagation velocity is so important in identifying the joint-driving mechanism, little is known about natural joint velocities. However, there are some facts and inferences that have a bearing on our analysis of driving mechanisms.

Experiments with glass show that, as crack propagation accelerates concurrently with an increase in stress intensity, the morphology of the crack surface progresses from a mirror surface to a mist and then to a hackle (Johnson and Holloway, 1966). Fractography of stress corrosion cracking in glass shows slow cracks to be smooth with crack arrest marked by slight irregularities (Michalske, 1994). In general, there is agreement in the ceramics literature (e.g., Mecholsky, 1994) that smooth surfaces are indicative of low stress intensities (i.e., slower velocities), that arrest leaves an irregularity called an arrest line, and that as the stress intensity increases (i.e., higher

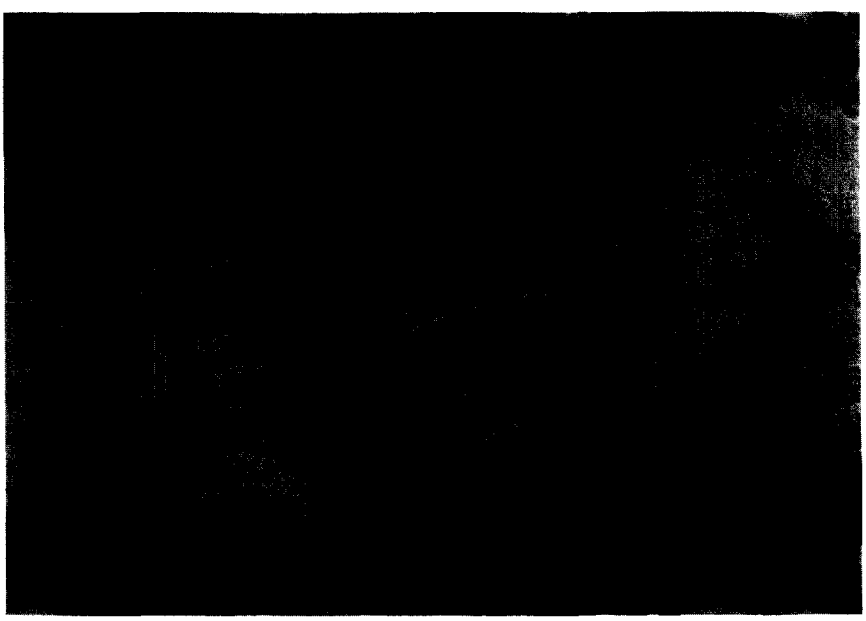

Fig. 4. A blast fracture on an outcrop face of the Ordovician Bellefonte Formation along Route 322 near State College, Pennsylvania, U.S.A. (Srivastava and Engelder, 1990). Rib marks indicate a fracture propagating from right to left with initiation within the irregular area on the right side of the field of view. Scale in the upper right is an American 5 cent piece.

velocities), cracking ahead of the crack front leads to branching and an irregular fracture surface. We will apply these general rules to our analysis of the propagation velocity of natural joints.

Measurement of in situ joint propagation velocity, V_p, is nearly impossible and we are unaware of any data on natural propagation velocity. However, some reasonable inferences are possible based on field observations. First, blast fractures propagate at a rate that may approach the shear wave velocity of the rock ($V_p > 10^3$ m/s). Rib marks on a conchoidal-like (i.e., nonplanar) surface are characteristic of the morphology of blast fractures (Fig. 4). Well-developed hackles are often found normal to the ribs. Rib marks are also common on the surface of mud cracks which propagate at a slower velocity than blast fractures (10^{-1} m/s $> V_p > 10^{-4}$ m/s) (Fig. 5). Like the transition from smooth to rough surfaces on ceramics, the rib marks on mud cracks are found after a period of growth characterized by smooth surfaces. The growth of hydraulic fractures within plexiglass produces rib marks (e.g., Rummel, 1987) where the crack propagation velocity is similar to that of mud cracks (10^{-2} m/s $> V_p > 10^{-3}$ m/s) (Freeman, 1991). The transition from subcritical to critical crack propagation for quartz takes place in this same range of crack velocities (10^{-2} m/s $> V_p > 10^{-3}$ m/s) (Atkinson, 1984). Henceforth, we refer to joint propagation velocity in the range of 10^{-3} m/s to 10^{-1} m/s as critical or slow propagation to distinguish it from subcritical propagation and supercritical propagation near the shear wave velocity of rock. Again, the observations suggest that slower cracks are smooth and those propagating between critical and supercritical velocities are most likely to develop an irregular morphology.

Sand dikes propagate when a sand–water slurry washes into a joint just as it is opening (Fig. 6). Because sand particles of 1 mm diameter settle in water at the rate of about 7 cm/s (Rubey, 1933), the slurry must wash into the open joint at a higher rate to keep the sand suspended. Assuming that the slurry washes into the joint at the rate of joint propagation, we infer that the joint must propagate with a minimum velocity of 10^{-1} m/s or the joint would not fill with a sand–water slurry. Although this is indi-

Fig. 5. Joint face on a mudcrack formed January 1995 in a sediment pond near Zafrana on the west bank of the Gulf of Suez, Egypt. Rib marks indicate a fracture propagating from right to left. A smooth mud crack surface with plume morphology is seen below the coin. Scale is an Egyptian 5 piaster piece.

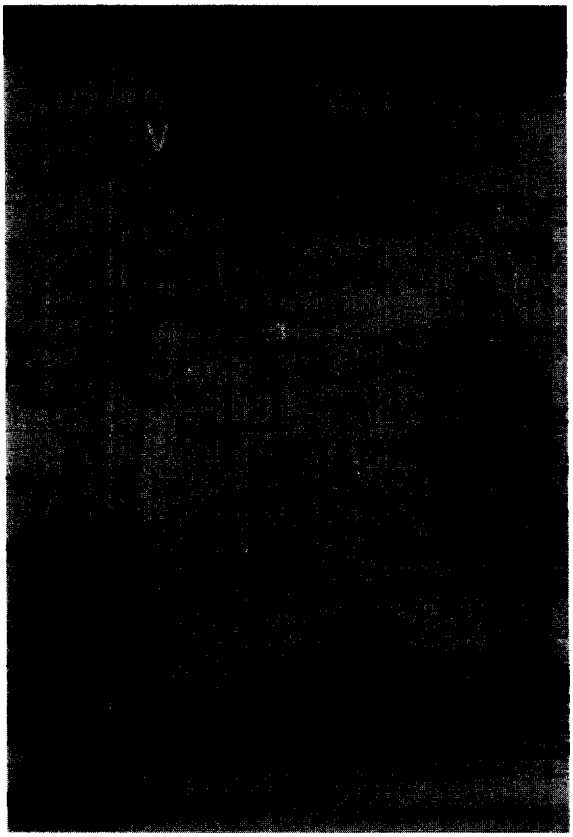

Fig. 6. A vertical sand-filled joint (white arrows) intrudes these steeply dipping beds of the Miocene Monterey Formation near Gaviota Beach west of Santa Barbara, California, U.S.A. (Gross, 1993).

rect evidence pointing to propagation rates at critical velocities, the surface morphology of joints filled by sand has, to our knowledge, never been observed.

Many natural joints in clastic sedimentary rocks like those of the Devonian Catskill Delta complex exhibit a very subtle plume surface morphology but are otherwise smooth and often planar on the scale of 1–2 m (i.e., Bahat and Engelder, 1984). If these joints curve there is usually clear evidence for some local perturbation of the crack-tip stress field. Other smooth-planar joints exhibit a fan-like pattern of very fine hackles that end abruptly indicating incremental propagation events (Lacazette and Engelder, 1992). This fan-like pattern repeats itself through many events indicating a stable joint whose growth may have accelerated just before arrest assuming a correlation between propagation velocity and surface roughness (Fig. 7). The smoothness of joint surfaces without sizable hackles, rib marks, or a conchoidal shape point to a slower propagation ($V_p < 10^{-1}$ m/s) just as the smooth surfaces of glass and ceramics are produced at slower velocities. Both rib marks (fig. 2.2 in Engelder, 1987) and coarse hackles (fig. 2.5 in Engelder, 1987) are found in the Devonian Catskill Delta complex but these higher velocity features are rare. Vein-filled joints in the Bellefonte Formation in the Appalachian Valley and Ridge also exhibit a subtle plume morphology (fig. 7a of Srivastava and Engelder, 1990). These vein-filled joints are also remarkably planar on the 1–2 m scale. With both the clastic rocks of the Catskill Delta complex and the carbonates of the Appalachian Valley and Ridge, there seems little doubt that lack of rib marks and coarse hackles is indicative of joint propagation at a steady, slow rate. Whether planarity is also indicative of subcritical propagation as well as slow propagation is less certain. However, in lieu of better data, we suspect that smooth, planar joint surfaces are indicative of propagation at speeds considerably less than the shear wave velocity of the rock.

4. Loading configurations and driving mechanisms

Having established a model for a rock-joint system in the context of the Griffith energy-balance concept, we now delineate four basic joint-loading configurations and their ancillary joint-driving mechanisms, and place each of them in a geological context. We define a joint-driving mechanism in terms of the sources of energy that are taken up by joint propagation. Joint-driving mechanisms should not be confused with a joint-driving stress, a quantity that denotes the effective stress at the initiation of joint propagation.

4.1. Joint-normal load

Our first treatment of Griffith's (1920, 1924) energy-balance concept will apply to joint propagation within rock above the water table or a rock where pore pressure is low. In these cases joints are loaded in a manner that resembles a dead-weight pull on a joint-parallel boundary. This configuration is called a

Fig. 7. Plumose morphology exhibiting the fan-like pattern indicative of repeated propagation and arrest in the Devonian Ithaca Formation along Route 414 east of Watkins Glen, New York, U.S.A. (Lacazette and Engelder, 1992).

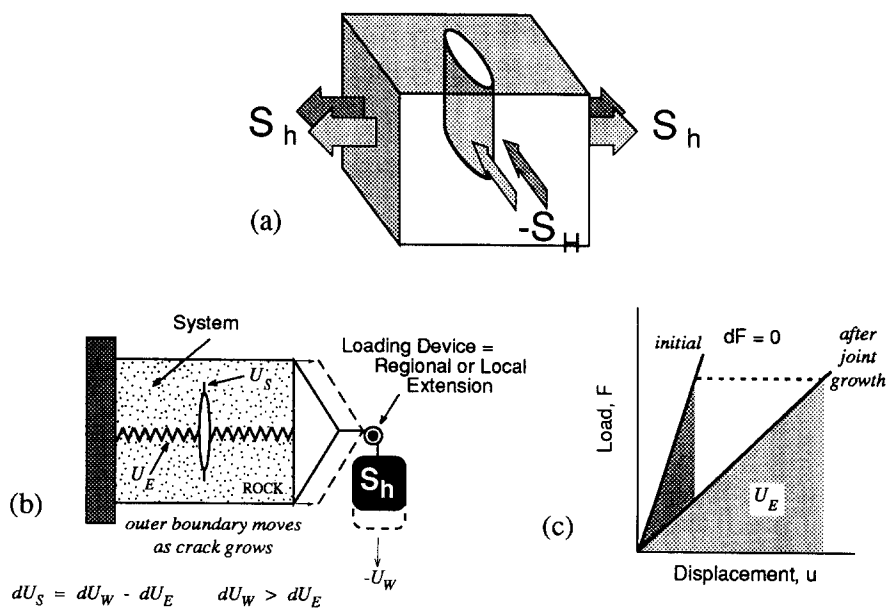

Fig. 8. Model for joint-normal loading. (a) Loading configuration for joint-normal loading of a vertical joint. Maximum and minimum horizontal stresses are given as $-S_H$ and S_h. (b) Thermodynamic energy balance diagram for the joint-driving mechanism, joint-normal stretching. (c) Schematic force-displacement graphs illustrating the amount of strain energy before (dark shade) and after (light shade) joint propagation. Rock modulus is the slope of the force-displacement curve. During joint propagation driven by joint normal stretching the rock modulus decreases and the strain energy (light shade) increases.

joint-normal load (Fig. 8a and b). In nature, three conditions must be satisfied for the release of energy under joint-normal loading. First, a joint-parallel boundary of the rock-joint system must move outward at a rate comparable to the rate of dilation of the joint during propagation. This is necessary to mimic the release of potential energy by the motion of a loading device. Certainly, rapid joint propagation ($V_p > 10^{-2}$ m/s) must exceed the capacity of the rock to extend under ordinary circumstances. To satisfy the condition of slow deformation, it seems that joint propagation velocity must be subcritical. Second, the crack wall must be stress-free or nearly so. Third, moisture is required for stress corrosion which is largely responsible for subcritical crack propagation (e.g., Atkinson, 1984). If these three conditions are satisfied, the joint-driving stress is approximately S_h because the fluid exerts little or no pressure on the joint wall.

During joint-normal loading work by the remote stress drives the joint. Upon joint propagation the potential energy, U_W, of the remote stress decreases (i.e., the rock extends during joint growth) while U_S within the rock increases with the formation of new joint surfaces. During joint propagation U_W and U_S are not constrained to balance. To maintain equilibrium, any difference in the changes of U_W and U_S is taken up by an appropriate change in U_E. Although work by the remote stress and elastic strain energy both contribute to a change in the mechanical energy of the system, they differ both in sign and magnitude when the rock-joint system is subject to joint-normal loading. As the joint propagates, the elastic modulus of the rock-joint system decreases (Broek, 1987), causing an increase in strain energy within the system (Fig. 8c). Because both U_S and U_E increase, a decrease in U_W must be larger than any increase in U_E. Thus, the joint-driving mechanism for joint-normal loading is the release of potential energy through work on an external boundary, part of which energy is accommodated by an increase in strain energy, and the other part taken by surface energy. This driving mechanism is called *joint-normal stretching*.

Numerous are field examples of joints driven by the release potential energy under the joint-normal stretching mechanism. We infer that joint-normal loading may occur in the outer arc of a fold where a remote stress causes the stretching of a rock layer. The more intense development of joints in the hinge of folds may reflect this joint-loading configuration

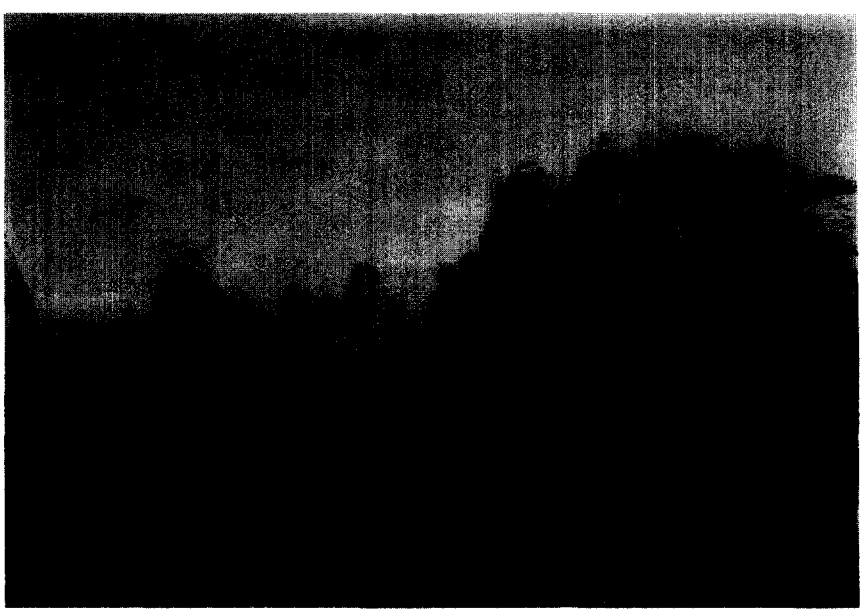

Fig. 9. The Moab Member of the Jurassic Entrada Formation near the Devil's Garden Campground in Arches National Park, Utah, U.S.A. The formation is cut by joint set J_1^A of Dyer (1988). The joints formed as the Entrada Formation was extended over a series of salt-cored anticlines of the Paradox Basin on the Colorado Plateau.

(e.g., Murray, 1968; Narr, 1991). The best candidates for such joints may be in near-surface folds such as those formed at Arches National Park, Utah (Fig. 9), where the consensus is that joints formed in response to a regional extension (Dyer, 1988; Cruikshank et al., 1991). While the velocity of propagation of these joints is unknown, their surface morphology is characterized by hackle and plumose structures (e.g., Cruikshank and Aydin, 1994) that are indicative of slow propagation ($V_p \ll 10^3$ m/s) in clastic rocks according to arguments stated previously. We note that if joints at Arches propagated below the water table, the joint driving stress had a component from pore pressure as noted in the Cruikshank et al. (1991) analysis. We address the action of pore water inside joints below.

A second situation where joint-normal stretching appears to be a driving mechanism that is found in the extension of layered sedimentary rocks at great depths ($z > 10$ km) where some rocks exhibit significant ductility and boudinage is an active process. The underside of Lebanon Valley nappe in the Appalachian Piedmont, Pennsylvania contains an Ordovician carbonate consisting of alternating layers of dolomite and limestone (Faill and Geyer, 1987). Here, ductile flow of the limestone layers exerts a traction on the stronger and more brittle dolomite beds causing these latter beds to joint at regular intervals (Fig. 10). The theoretical explanation for stretching and boudinage is extensively treated in the literature (e.g., Masuda and Kuriyama, 1988).

In examples of boudinage there is little doubt that the rate of extension is slow. The question is whether jointing (i.e., vein growth) was equally slow, as is necessary for the joint-normal stretching driving mechanism. Two types of textures are observed in veins which may indicate the propagation rate. The characteristics of displacement-controlled fibers suggest that development of veins involves transport-limited growth along a cohesive matrix-vein face (Fisher and Brantley, 1992). Here the veins grow at the rate of extension as is required for joint-normal stretching. If joint growth is fast, fluid pressure would have to prop veins open until mineral growth can support vein walls. Evidence from face-controlled quartz veins suggests that propagation is rapid relative to extension for these veins (Fisher and Brantley, 1992).

Joint-normal stretching associated with a ductility contrast is not limited to bedded sedimentary se-

Fig. 10. Interbedded dolomite and limestone in the Ordovician Eppler Formation exposed in the Rheems Quarry near Elizabethville, Pennsylvania, U.S.A. (Faill and Geyer, 1987). Joints in a dolomite bed are infilling with calcite.

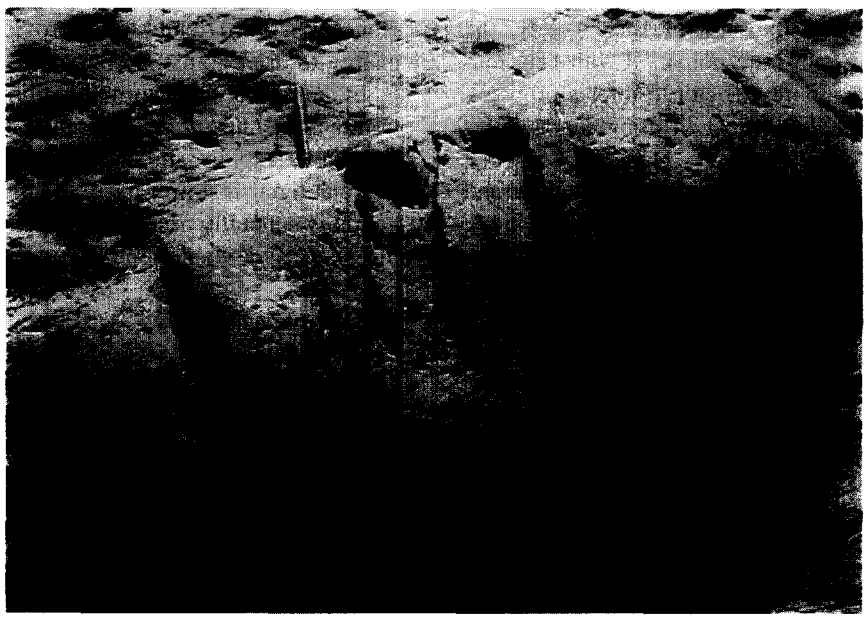

Fig. 11. The Pennsylvanian Llewellyn Formation in Bear Valley Strip Mine, Pennsylvania, U.S.A. (Nickelsen, 1979). This formation of anthracite grade coal, fluvial sandstone, mudstone, and clayey shale contains large ironstone concretions on the order of a meter in diameter. Pen for scale. This figure shows Stage II, Early Alleghanian, northwest-striking systematic joints cutting an ironstone concretion.

quences. For example, jointed ironstone concretions are surrounded by sandstone within the Bear Valley strip mine of the anthracite region in the Appalachian Valley and Ridge, Pennsylvania (Nickelsen, 1979). Here, layer-parallel extension led to joint propagation through the stiffer and more brittle con-

Fig. 12. Interbedded dolomite and shale of the Miocene Monterey Formation exposed on the shoreline of the Pacific Ocean near Vandenburg Air Force Base, California (Gross et al., 1995).

cretions (Fig. 11). In the case of Bear Valley, the concretion-cutting joints are not filled with vein material and thus it is more difficult to infer a propagation velocity, a factor critical in assigning a joint-driving mechanism.

Joint spacing in bedded sediments is regular and approximately proportional to bed thickness (Price, 1966). Such a joint spacing–bedding thickness relationship is found in the Monterey Formation along the Santa Barbara Channel area of California (Fig. 12). This relationship is largely controlled by the local tensile stress normal to each joint which is reduced in the vicinity of the joint because such stresses are not transmitted across free surfaces (Gross et al., 1995). Here again is an example where the rate of joint propagation is unknown although the joints are smooth with little tendency to show rib marks or conchoidal surfaces. If they propagate at subcritical velocities and if pore water pressure was low upon propagation, joint-normal stretching is a viable driving mechanism. While jointing in the Monterey formation is associated with folding (Narr, 1991), a regional stretching during the uplift of sedimentary rocks (e.g., Price, 1974; Bevan and Hancock, 1986) could also provide the necessary energy to drive joints in cratonal basins.

In summary, joint-normal loading is a configuration that operates in the laboratory where boundaries can move rapidly. In the field, where boundaries move at a much slower pace, subcritical crack propagation is generally necessary for joint-normal stretching to act as a viable joint-driving mechanism.

4.2. Thermoelastic load

Another loading configuration for in situ joint propagation arises when the loading device does not displace during joint propagation. This is known as 'fixed-grips' loading and the correlative natural configuration is called a *thermoelastic load* (Fig. 13a and b). One distinction between joint-normal and thermoelastic loading is in the behavior of stress at a joint-parallel boundary. In a laboratory experiment subject to 'fixed-grips' loading, tensile stress at the loading device on the specimen (i.e., the external boundary) decreases during joint propagation. Under dead-weight loading, tensile stress at the loading device does not change during joint propagation.

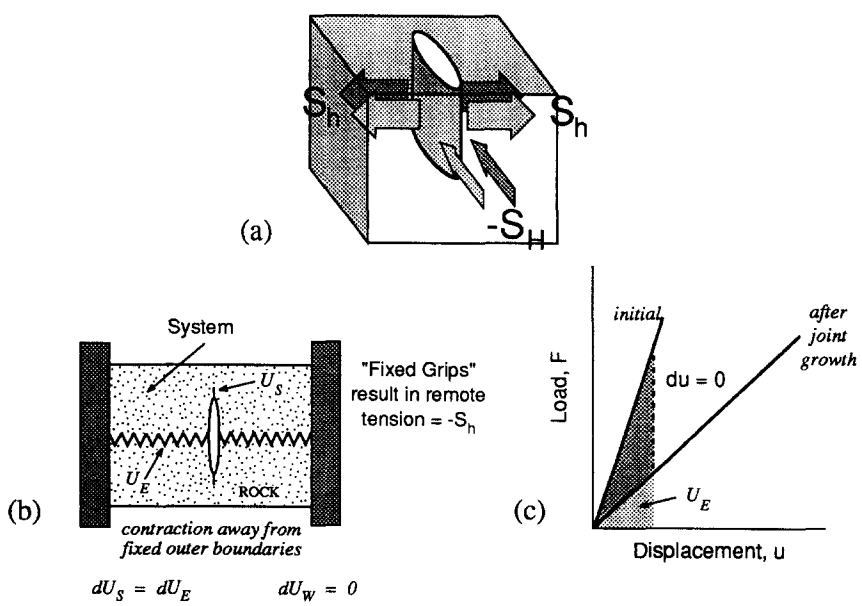

Fig. 13. Model for thermoelastic loading. (a) Loading configuration for thermoelastic loading of a vertical joint. Maximum and minimum horizontal stresses are given as $-S_H$ and S_h. Fixed boundaries are shaded. (b) Thermodynamic energy balance diagram for the joint-driving mechanism, thermoelastic contraction. (c) Schematic force-displacement graphs illustrating the amount of strain energy before (dark shade) and after (light shade) joint propagation. Rock modulus is the slope of the force-displacement curve.

Thermoelastic loading may be more germane to in situ joint propagation than joint-normal loading because fast joint propagation (i.e., propagation under a stress intensity at or near the critical stress intensity) does not allow time for a remote boundary to move. Individual jointing episodes may be interrupted by long periods of time during which remote boundaries may extend slowly. During these periods of extension, work at remote boundaries is transformed to strain energy within the rock-joint system. Thermoelastic loading may occur during cooling of hot rocks or during unloading upon uplift and erosion. In each case, joints are driven by the release of elastic strain energy through a mechanism we call *elastic contraction*.

Upon joint propagation under thermoelastic loading, the loading device (i.e., a remote boundary) remains fixed and, therefore, does not contribute work, U_W, toward the generation of new surface area. The rock-joint system is not sensitive to whether the joint driving stress was generated by slow extension or thermoelastic deformation. Presumably, there is no load on the inside of the joint as a consequence of fluid pressure. Like joint-normal stretching, the joint-driving stress is S_h, but this stress arises as a consequence of slow extension, thermoelastic cooling, or elastic rebound upon erosion. Because $dU_W = 0$ under elastic contraction, the only component of mechanical energy available to drive a joint is U_E, which must decrease while U_S increases during joint growth within the rock. To maintain equilibrium during joint propagation, $dU_E = dU_S$. A decrease in U_E arises as a consequence of the decrease in both load and elastic modulus during crack propagation (Fig. 13c). Elastic contraction is the only joint-driving mechanism where the energy release for joint propagation comes solely from elastic strain energy.

In nature, tensile stresses can develop in response to thermoelastic loading during cooling or during uplift and erosion, where the removal of overburden stress favors lateral contraction. Cracks formed due to cooling include columnar joints (Fig. 14), where each column forms by the incremental growth of joints from the cool exterior to the hot interior of the basalt flow (DeGraff and Aydin, 1987). Each increment is characterized by a delicate plume morphology of hackles paralleling the direction of crack propagation. These joints are smooth but show a curved surface where the joint was subject to mixed-mode loading during propagation. Because each increment is of limited area and shows the smooth surface, propagation velocity was probably slow if not subcritical. We argue that a release of strain energy drove these joints because they formed in response to elastic contraction rather than stretching under a remote stress. The adjective, elastic, applies rather than thermoelastic because joint propagation was fast relative to the cooling rate of the basalt.

Fig. 14. Snake River Basalt flow along the Boise River at Lucky Peak Dam, Idaho (adapted from DeGraff and Aydin, 1987). The formation carried a columnar joint set with the column faces showing bands of incremental propagation oriented normal to the vertical column axes. Photo courtesy of A. Aydin.

Mud cracks display the same axial symmetry as columnar joints (Fig. 15). During propagation, remote boundaries are fixed so it is reasonable to conclude that mud cracks are also driven by elastic contraction. Although the mechanism for contraction

Fig. 15. Mud cracks forming in a sediment pond near Zafrana on the west bank of the Gulf of Suez, Egypt. The milk carton triggered crack propagation radiating away from the carton with hexagonal symmetry.

was desiccation rather than cooling, the surface energy for joint propagation comes from the release of strain energy within the drying mud.

Granite plutons of the New England region, U.S.A., contain a microcrack fabric that exhibits the same orientation over large regions encompassing

Fig. 16. A thin section of a hornblende gneiss near Blue Mountain Lake in the Adirondack Mountains, New York, U.S.A. This sample comes from site #6 reported in Plumb et al. (1984b). Within the gneiss are ENE-striking transgranular and intragranular microcracks.

many plutons of similar age (Dale, 1923). The plane of these aligned microcracks is referred to as the granite's rift. Although these microcracks are not joints in the strict sense, they propagate under the same joint-driving mechanism. The alignment of these microcracks over large regions is indicative of a regional stress field at the time of cracking with the normal to these microcracks facing the direction of the least principal stress (Plumb et al., 1984a). Thermoelastic loading after intrusion of these granites is the mechanism for generating the tensile driving stress for these microcracks. Such rift planes are common in many crystalline rocks regardless of mineralogical composition including those of considerable age (Fig. 16).

Whether regional stretching occurs upon uplift is a matter of debate. Erosion alone will cause elastic contraction and the propagation of joints in the presence of the contemporary tectonic stress field (e.g., Hancock and Engelder, 1989). Another interpretation of cross joints (Fig. 17) is that they grow in response to a elastic contraction in near-surface rocks (Engelder and Gross, 1993).

Like joint-normal loading, ideal thermoelastic loading applies only when the joint is subject to little or no internal load from fluids. While this loading configuration may be common during the initial stages of cooling of an igneous intrusion, it may be supplemented by fluid loading during the propagation of joints forming upon uplift late in the orogenic cycle. Although elastic contraction is a mechanism driving cracks relatively fast cracks and joints, subcritical velocities may also be common with this driving mechanism.

4.3. Fluid load

The third application of the Griffith energy-balance concept to rocks is a solution to the old paradox that 'tensile' joints propagate within a highly compressive stress field such as that found at great depth. Crosby (1882) argued that tensile stresses did not exist in deeply buried rocks because heat and the enormous pressure of the overlying strata caused lateral expansion and prevented the contraction necessary for crack propagation. Later Secor (1965) proposed that joints could develop at great depths in the crust of the earth in the presence of a fluid pressure at or near the magnitude of the least compressive rock stress. The boundary conditions for the

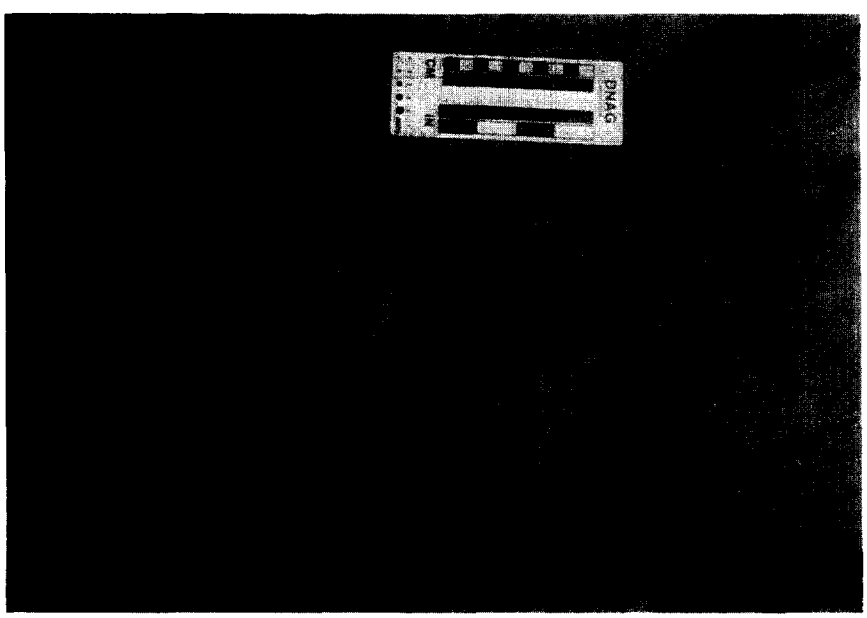

Fig. 17. The Miocene Monterey Formation near Alegria Beach, California (Gross, 1993). Curvy cross joints propagate between the initial strike-perpendicular joints.

type of crack propagation envisioned by Secor (1965) involve a fluid pressure (i.e., a 'dead-weight' load) on the joint wall. Because either liquids or gases can operate to drive a joint, the joint-loading configuration is called *fluid loading* (Fig. 18a and b). Joints propagating under this loading configuration are commonly called natural-hydraulic fractures (Secor, 1969; Engelder and Lacazette, 1990).

Joint propagation velocity has a great bearing on our analysis of fluid loading. First, we examine the case where propagation is relatively fast ($V_p \approx 10^{-3}$ m/s) and possibly critical ($V_p > 10^{-1}$ m/s). Here, the remote, joint-parallel boundaries of the rock-joint system are unlikely to displace significantly during the propagation event. This is analogous to a fixed-grips loading configuration in which case the rock-joint system does no work against remote $-S_h$ during joint propagation. Despite a fixed outer boundary, the driving mechanism is more complex than for elastic contraction, because a 'dead-weight'-like loading configuration exists in the form of fluid pressure on the crack wall. Under such conditions, where work is done on the rock-joint system by the internal fluid, the sign of the potential energy term in Eq. (7) remains negative.

With the buildup of pore pressure the joint walls may start to part because of poroelastic contraction. Crack propagation does not start under the influence of internal pressure within the crack, P_i, until there is a net outward force when $P_i > |-S_h|$. The change in U_E during joint propagation depends on both the movement of the joint wall and on the change in net outward force or effective stress within the joint. When the joint wall moves in response to joint

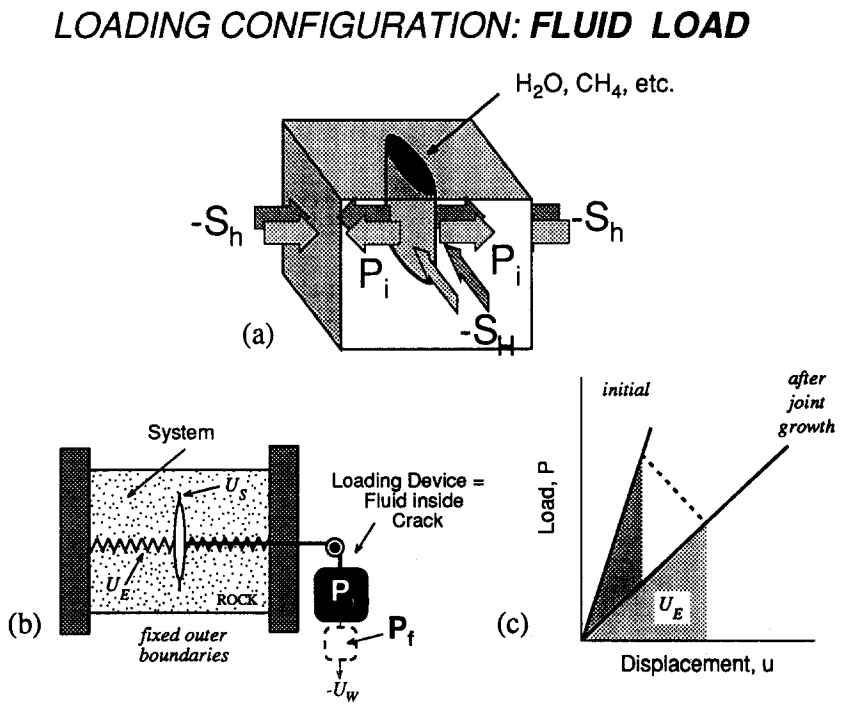

Fig. 18. Model for the joint-loading configuration, fluid loading. (a) Stress configuration for fluid loading of a vertical joint. Maximum and minimum horizontal stresses are given as $-S_H$ and $-S_h$ and initial pore pressure is P_i. Fixed boundaries are shaded. (b) Thermodynamic energy balance diagram for the joint-driving mechanism, fluid decompression. The initial pore pressure is P_i and the final pore pressure is P_f. (c) Schematic force-displacement graphs illustrating the amount of strain energy before (dark shade) and after (light shade) joint propagation. Rock modulus is the slope of the force-displacement curve.

propagation, there is a decrease in potential energy of the loading device, the fluid. The system is subject to a combination of dead-weight and fixed-grip loading configurations. A change in U_W given up by the system (to reduce the pore pressure) is balanced by changes in U_S and U_E in the rock. Because fluid pressure decreases during rapid joint propagation, the load is not a dead weight per se. Depending on the change in modulus of the rock upon joint propagation and the amount of pore pressure change within the joint, U_E can increase, decrease, or under unusual circumstances not change at all (Fig. 18c). *Fluid decompression* is the joint-driving mechanism where the energy released for formation of new joint surface area can come from both a change in potential energy of the driving fluid and a decrease in strain energy within the rock.

Examples of rock cracks interpreted to have been driven by an internal pressure include joints (Secor, 1965, 1969), dikes (e.g., Delaney et al., 1982; Elsworth and Voight, 1992), and veins (e.g., Beach, 1977; Ramsay, 1980). In his seminal papers on natural hydraulic fracturing Secor (1965) suggested that incremental propagation of joints indicates fluid-driven jointing. Other evidence for an internal fluid drive comes from the association of joint propagation with episodes of increased fluid pressure (Laubach, 1988), and kerogen/bitumen laminae in petroleum source rocks (Lehner, 1990).

Many of our inferences about fluid loading of natural joints come from the Appalachian Plateau. Such evidence as undercompaction (Engelder and Oertel, 1985; Oertel et al., 1989), poroelastic relaxation (Evans et al., 1989b), and fluid inclusion trapping pressure (Srivastava and Engelder, 1991; Evans, 1994) all point to an abnormal pressure event during the Alleghanian orogeny in the Appalachian Basin. Morphologic evidence for a fluid drive comes from individual joints that have grown through more than 60 increments in as much as 28 m (Lacazette and Engelder, 1992). The increments are subtle fan-shaped features with slightly coarser hackle in front of an arrest line (Fig. 7). Many of these joints are confined to individual beds whereas in other cases the incremental morphology is restricted to one bed within a composite joint (Helgeson and Aydin, 1991). Incremental propagation occurs because the rate of fluid or gas leakage from the matrix to the joint is slower than the propagation of the joint. Arrest occurs because a liquid or gas decompresses on joint growth and this causes a drop in the joint driving stress. The joint-driving mechanism is a fluid decompression which may be a combination of loss of potential energy in the fluid and a release of strain energy in the rock. Clastic dikes are excellent examples of fluid-driven jointing (Fig. 6). Fluid drive is certainly required for the formation of these structures.

During subcritical crack propagation, pore fluid may infiltrate the joint to maintain a load which does not fluctuate during joint propagation. In this case, the load is a dead weight in the strict sense and we call the joint-driving mechanism, *fluid drive*. Because the load is maintained throughout subcritical crack propagation, the work by the fluid may seem higher than for cyclic joint propagation at higher pressures. However, the absolute magnitude of the surface traction comes into play in fluid loading. More work is contributed by fluid loads during the fast growth of joints because the average fluid pressure is generally higher.

Subcritical crack propagation ($V_p \ll 10^{-3}$ m/s) under fluid loading is most likely to occur during slow intrusion of magma. While both the intrusion of magma as dikes and infiltration of pore fluid into joints constitute examples of the buildup of joint-driving stress, the joint (or dike)-driving mechanism is somewhat different from the fluid decompression mechanism. Magma is relatively incompressible and, thus, less likely to drive joints by volumetric expansion upon decompression. Magma pressure is maintained by feeder dikes connecting to a larger magma chamber. The pressure on the dike walls may not cycle during magma intrusion but rather act as a true dead-weight load with intrusion keeping pace with slow dike propagation. In contrast, some joints show a surface morphology consistent with pressure relaxation due to decompression of fluids along joints (e.g., Lacazette and Engelder, 1992). In the former case work by magma may drive the dike whereas in the latter case the release of strain energy may play a role.

In principle, all three Griffith energy terms come into play for the fluid decompression, fluid-drive, and joint-normal stretching driving mechanisms. The difference among these joint-driving mechanisms is

the boundary on which the loading device acts. Fluid decompression and fluid drive are mechanisms where the loading device, pore fluid, acts on an internal boundary of the rock-joint system and U_E may increase or decrease depending on the situation, whereas for joint-normal stretching the loading device (e.g., remote stresses about a fold) acts on an external boundary of the system and U_E always increases during joint propagation (compare Fig. 8c and Fig. 18c).

4.4. Axial loading

The fourth application of the Griffith energy balance to define a joint-loading configuration is the only example where either elastic strain energy or a dead weight load, $-S_H$, operates parallel to the joint. In laboratory experiments where specimens fail by cracking parallel to the applied compressive load, this behavior is often called axial splitting and the loading configuration is called an *axial load* (Fig. 19a and b).

The phenomenon of axial splitting is most often explained in terms of the propagation of wing cracks from the tips of 'Griffith' flaws (e.g., microcracks, grain boundaries) in rock (Fig. 19b; Nemat-Nasser and Horii, 1982; Horii and Nemat-Nasser, 1985; Ashby and Hallam, 1986). Because stress is not concentrated at the tips of sharp flaws aligned parallel to a compressive stress field, crack propagation in compressive stress fields occurs by a frictional sliding along pre-existing flaws in a material (McClintock and Walsh, 1963; Ashby and Hallam, 1986). Experiments in glass by Brace and Bombolakis (1963) and Hoek and Bieniawski (1965), in Columbia resin CR39 by Nemat-Nasser and Horii (1982) and Horii and Nemat-Nasser (1985), and in PMMA (polymethelmethelacrylate) by Ashby and Hallam (1986) all show that tensile cracks (i.e., wing cracks) grow from the tips of initial flaws oriented at some angle ($0 < \theta < 90°$) to a uniaxial compressive stress field. Wing cracks initiate at some angle to the parent flaw and extend in the direction parallel to the maximum compressive stress, resulting in a curvilinear crack shape. Similar wing crack growth is observed for angled cracks subjected to tensile loads and this behavior is well understood and predicted by the principles of linear elastic fracture mechanics (Erdogan and Sih, 1963; Cotterell and Rice, 1980). The crack-driving stress for wing cracks is the local tensile stress which develops at the tip of an inclined flaw undergoing mode II deformation (Lawn and Wilshaw, 1975).

The configuration for axial loading suggests that neither the crack-parallel boundary nor the internal wall of the crack is loaded. As a consequence there is no accumulation of crack-normal strain and its accompanying strain energy. To maintain equilibrium, two situations are possible for a joint driving mechanism which we call *axial shortening*. In the first situation, an increase in U_S is counterbalanced by a drop in potential energy because remote boundaries move as the axial load loses potential energy during joint propagation. In the second situation,

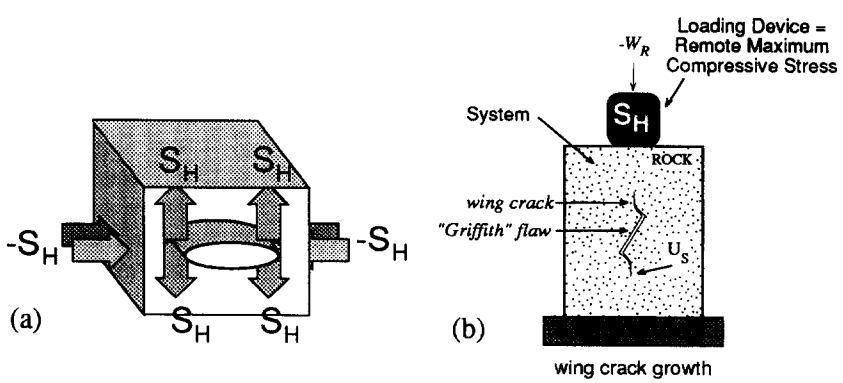

Fig. 19. Model for the joint-configuration, axial loading. (a) Stress configuration for a horizontal joint (e.g., sheet fracturing). Maximum horizontal stress is given as $-S_H$. (b) Thermodynamic energy balance diagram for wing crack mechanism of axial splitting. The joint-driving mechanism is axial splitting.

joint propagation is so rapid that strain energy is released to drive the joint.

Sheet fractures are often cited as natural examples of axial splitting (Holzhausen and Johnson, 1979). Other names for these joints are exfoliation fractures or longitudinal fractures. In nature they propagate parallel to the Earth's surface which may either be subhorizontal or sloping steeply as is the case for the famous sheet fractures of the Half Dome structure of Yosemite Park, California, U.S.A.. Circumstances leading to their propagation include the removal of overburden which leads to a joint-normal stress approaching zero and a relatively high horizontal stress which is a common feature of near surface rocks (e.g., Plumb et al., 1984a). Sheet fractures must be driven by an axial load because the presence of a free surface overlying the joints excludes any possibility of a tensile joint-normal load. The genetic connection between sheet fractures and the near surface environment is indicated by the increased spacing between sheet fractures with depth of burial (Fig. 20). With depth, joint-normal loading becomes increasingly compressive and acts to suppress propagation of axial splitting cracks.

Axial shortening may lead to propagation of microcracks and mesoscopic cracks of modest size ($2c \ll$ m). However, significant extension of such cracks at depth is unlikely because the crack-normal confining stress tends to suppress the growth of long wing cracks. In laboratory experiments, such crack growth more often leads the development of an extensive set of axial microcracks that eventually coalesce into a fault. In nature, short axial splitting cracks are common in cataclastic rock where grain–grain contacts lead to microcracking (Gallagher et al., 1974). One of the characteristics of cataclastic

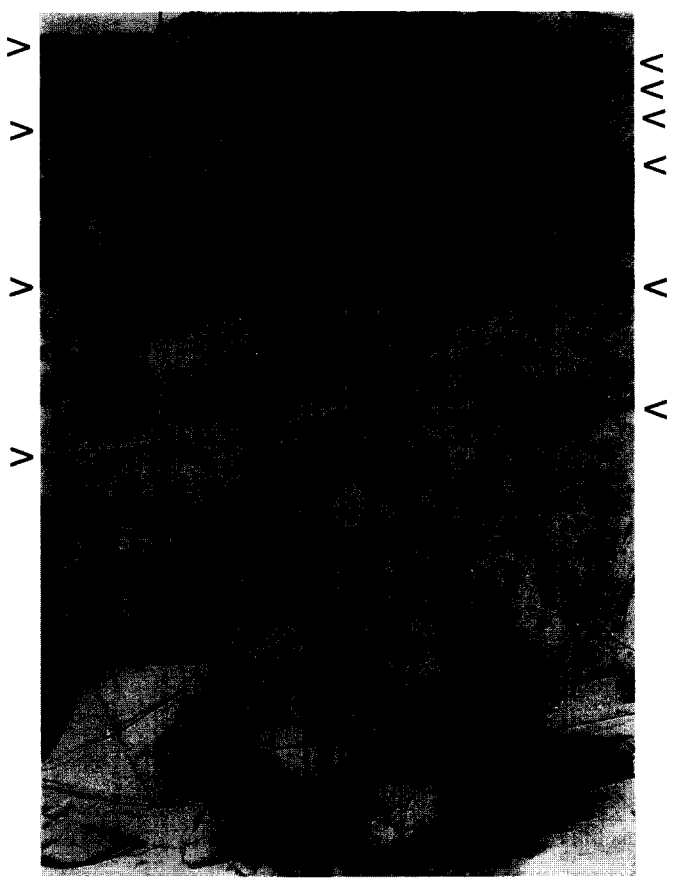

Fig. 20. Sheet fractures within the Algerie Granite in the Williams Stone Quarry near East Otis, Massachusetts, U.S.A. (Engelder, 1984).

Fig. 21. A thin section of cataclastic rock from the Towaliga Fault in Lamar County, Georgia (Steltenpohl, 1988).

behavior is that a microscopic stress is so inhomogeneous that microscopic axial splitting weakens any fabric that might develop (Fig. 21). Rolling of grains in a cataclastic fault gouge further weakens any cataclastic microcrack fabric which might have developed (Engelder, 1974). On a larger scale, clast-to-clast contacts in a conglomerate lead to the same type of cataclastic fabric as seen on a microscopic

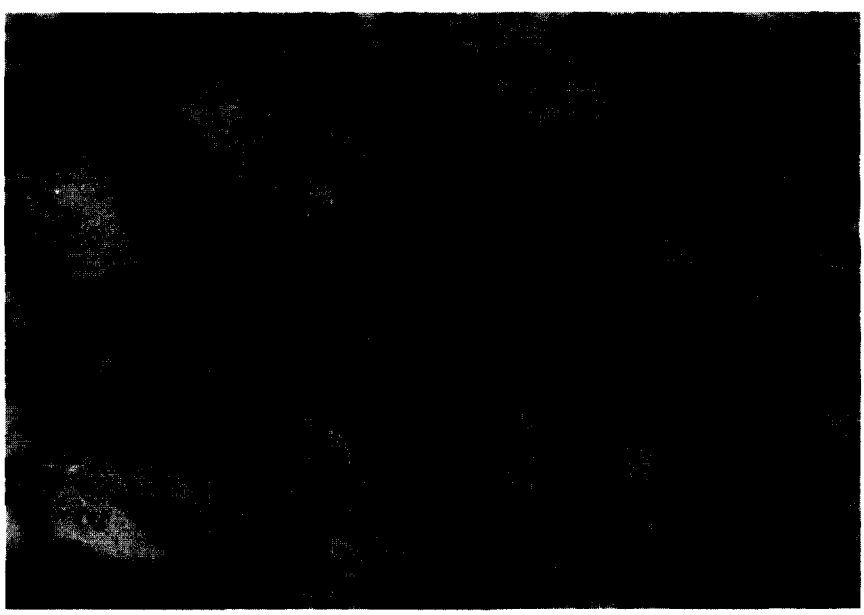

Fig. 22. A conglomerate showing grain–grain contact fractures. This sediment is found on the northern edge of a basin fill known as the Paleozoic of Austria. The scale is an Austrian 10 schilling piece.

scale. This fabric is commonly found in conglomerates that are caught within a fault zone (Fig. 22). Axial shortening is the crack driving mechanism responsible for such extensive cracking.

4.5. Summary comments

The four natural joint-loading configurations are ideal end members in a vast spectrum. In many cases a combination of configurations is the most likely during the propagation of a natural joint. The same may be said for joint-driving mechanisms. In all cases, the relative rates of joint propagation and deformation are closely associated with joint-driving mechanisms. For example, individual joint propagation events may occur so fast relative to joint-normal extension that outer boundaries do not displace during the short interval of joint propagation. If so, although the long-term (i.e. time-integrated) joint-driving mechanism is joint-normal stretching, the instantaneous joint-driving mechanism is closer to an elastic contraction. Axial splitting may work with either elastic contraction or joint-normal stretching to drive cracks through a combination of tensile and compressive stresses. Finally, the abundance of pore fluid in rocks suggests that either fluid decompression or fluid drive are very common joint-driving mechanisms acting to form natural joints.

5. Conclusions

Natural joint propagation occurs by the conversion of mechanical energy to surface energy under one of several loading configurations including a joint-normal load, a thermoelastic load, a fluid load, and an axial load. Each loading configuration releases mechanical energy through a joint-driving mechanism. Joint-normal loading is the natural analog to laboratory dead-weight loading and the joint-driving mechanism, joint-normal stretching, is the energy release through the loss of potential energy of the dead-weight. Elastic loading is the natural analog to laboratory fixed-grips loading and the joint-driving mechanism, elastic contraction, is the release of elastic strain energy. Fluid loading can act to drive either fast joint growth or subcritical crack propagation and is, perhaps, the most common of the joint driving mechanisms in the crust. The work necessary for the extension of a joint wall under fluid load is energy generated by a dead-weight configuration. Here the two joint driving mechanisms are fluid decompression and fluid drive, respectively. Axial loading can drive joints by the axial shortening mechanism which may involve either the release of potential energy of a load parallel to the joint-propagation direction or the release of elastic strain energy.

Acknowledgements

While at Yale, Neville Carter taught G&G 220a, a class titled 'Experimental Rock Deformation'. During this class in the fall of 1968 Neville first introduced T.E. to geological rock mechanics and A.A. Griffith's work. Because of this class, Neville is arguably the most influential person in heading T.E. towards a lifetime's fun dealing with many weighty questions concerning the in situ propagation of joints. Discussions with M. Gross, S. Loewy, D. McConaughy, and A. Younes were important in sharpening ideas for this paper. We also thank S. Choeng, S. Van Gundy, S. Ouyang, M. Everett, and B. Carson for reading early drafts. D. Secor's, and S. Laubach's careful reviews are also greatly appreciated. This work was supported by Penn State's Seal Evaluation Consortium (SEC).

References

Ashby, M.F. and Hallam, S.D., 1986. The failure of brittle solids containing small cracks under compressive stress states. Acta Metal., 34: 497–510.

Atkinson, B.K., 1984. Subcritical crack growth in geological materials. J. Geophys. Res., 89: 4077–4114.

Bahat, D. and Engelder, T., 1984. Surface morphology on cross-fold joints of the Appalachian Plateau, New York and Pennsylvania. Tectonophysics, 104: 299–313.

Barker, L.M., 1984, Specimen size effects in short-rod toughness measurements. In: Chevron-Notched Specimens: Testing and Stress Analysis. ASTM STP 855, Am. Soc. Test. Mater., pp. 117–133.

Beach, A., 1977. Vein arrays, hydraulic fractures, and pressure solution structures in a deformed flysch sequence, S.W. England. Tectonophysics, 40: 201–225.

Bevan, T.G. and Hancock, P.L., 1986. A late Cenozoic regional mesofracture system in southern England and northern France. J. Geol. Soc. London, 143: 355–362.

Brace, W.F. and Bombolakis, E.G., 1963. A note on brittle crack growth in compression. J. Geophys. Res., 68: 3709–3713.

Broek, D., 1987. Elementary Engineering Fracture Mechanics. Martinus Nijhoff, Boston, MA, 516 pp.

Bueckner, H.F., 1958. The propagation of cracks and the energy of elastic deformation. J. Appl. Mech., 80: 1225–1230.

Cotterell, B. and Rice, J.R., 1980. Slightly curved or kinked cracks. Int. J. Fract., 16: 155–169.

Crosby, W.O., 1882. On the classification and origin of jointed structures. Proc. Boston Soc. Nat. Hist., 22: 72–85.

Cruikshank, K.M. and Aydin, A., 1994. Role of fracture localization in arch formation, Arches National Park, Utah. Geol. Soc. Am. Bull., 106: 879–891.

Cruikshank, K.M., Zhao, G. and Johnson, A.M., 1991. Analysis of minor fractures associated with joints and faulted joints. J. Struct. Geol., 13: 865–886.

Dale, T.N., 1923. The commercial granites of New England. U.S. Geol. Surv., Bull. 738, 488 pp.

DeGraff, J.M. and Aydin, A., 1987. Surface morphology of columnar joints and its significance to mechanics and direction of joint growth. Geol. Soc. Am. Bull., 99: 605–617.

Delaney, P.T., Pollard, D.D., Ziony, J.I. and McKee, E.H., 1982. Field relations between dikes and joints: Emplacement processes and paleostress analysis. J. Geophys. Res., 91: 4920–4938.

Dyer, R., 1988. Using joint interactions to estimate paleostress ratios. J. Struct. Geol., 10: 685–699.

Elsworth, D. and Voight, B., 1992. Theory of dike intrusion in a saturated porous solid. J. Geophys. Res., 97: 9105–9117.

Engelder, T., 1974. Cataclasis and the generation of fault gouge. Geol. Soc. Am. Bull., 85: 1515–1522.

Engelder, T., 1984. The time-dependent strain relaxation of Algerie Granite. Int. J. Rock Mech. Min. Sci., 21: 63–73.

Engelder, T., 1987. Joints and shear fractures in rock. In: B. Atkinson (Editor), Fracture Mechanics of Rock. Academic Press, Orlando, pp. 27–69.

Engelder, T. and Gross, M., 1993. Curving cross joints and the neotectonic stress field in eastern North America. Geology, 21: 817–820.

Engelder, T. and Lacazette, A., 1990. Natural hydraulic fracturing. In: N. Barton and O. Stephansson (Editors), Rock Joints. A.A. Balkema, Rotterdam, pp. 35–44.

Engelder, T. and Oertel, G., 1985. The correlation between undercompaction and tectonic jointing within the Devonian Catskill Delta. Geology, 13: 863–866.

Erdogan, F. and Sih, G.C., 1963. On the crack extension in plates under plane loading and transverse shear. J. Basic Eng., 85: 519–527.

Evans, K., Oertel, G. and Engelder, T., 1989. Appalachian Stress Study, 2. Analysis of Devonian shale core: some implications for the nature of contemporary stress variations and Alleghanian deformation in Devonian rocks. J. Geophys. Res., 94: 1755–1770.

Evans, M.A., 1994. Joints and décollement zones in the Middle Devonian Shales: evidence for multiple deformation events in the central Appalachians. Geol. Soc. Am. Bull., 106: 447–460.

Faill, R.T. and Geyer, A.R., 1987. Rheems quarry; the underside of a Taconian nappe in Lancaster County, Pennsylvania. In: D. Roy (Editor), Geol. Soc. Am. Centennial Field Guide, Northeastern Section, pp. 51–54.

Fisher, D.M. and Brantley, S.L., 1992. Models of quartz overgrowth and vein formation: deformation and episodic fluid flow in an ancient subduction zone. J. Geophys. Res., 97: 20,043–20,061.

Freeman, A.L., 1991. Ice fracturing: a new method of rock excavation. Ph.D. Thesis, The Pennsylvania State University, University Park, PA, 83 pp.

Gallagher, J.J., Friedman, M., Handin, J. and Sowers, G., 1974. Experimental studies relating to microfracture in sandstone. Tectonophysics, 21: 203–247.

Griffith, A.A., 1920. The phenomena of rupture and flow in solids. Philos. Trans. R. Soc. London, A, 221: 163–198.

Griffith, A.A., 1924. Theory of rupture. Proc. First International Congress Applied Mechanics, Delft, pp. 55–63.

Gross, M.R., 1993. The origin and spacing of cross joints: examples from the Monterey Formation, Santa Barbara coastline, California. J. Struct. Geol., 15: 737–751.

Gross, M.R., Fischer, M.P., Engelder, T. and Greenfield, R.J., 1995. Factors controlling joint spacing in interbedded sedimentary rocks: integrating numerical models with field observations from he Monterey Formation, USA. In: M.S. Ameen (Editor), Fractpography: fracture topography as a tool in fracture mechanics and stress analysis. Geol. Soc. London, Spec. Publ., 92: 215–233.

Hancock, P.L. and Engelder, T., 1989. Neotectonic joints. Geol. Soc. Am. Bull., 101: 1197–1208.

Helgeson, D. and Aydin, A., 1991. Characteristics of joint propagation across layer interfaces in sedimentary rocks. J. Struct. Geol., 13: 897–911.

Hoek, E. and Bieniawski, Z.T., 1965. Brittle fracture propagation in rock under compression. Int. J. Rock Mech. Min. Sci., 3: 137–155.

Holzhausen, G.R. and Johnson, A.M., 1979. Analyses of longitudinal splitting of uniaxially compressed rock cylinders. Int. J. Rock Mech. Min. Sci., 16: 163–177.

Horii, H. and Nemat-Nasser, 1985. Brittle failure in compression: Splitting, faulting and brittle–ductile transition. Philos. Trans. R. Soc. London, 319: 337–374.

Jaeger, J.C. and Cook, N.G.W., 1969. Fundamentals of Rock Mechanics. Methuen and Co., London, 513 pp.

Johnson, J.W. and Holloway, D.G., 1966. On the shape and size of the fracture zones on glass fracture surfaces. Philos. Mag., 14: 731–743.

Lacazette, A. and Engelder, T., 1992. Fluid-driven cyclic propagation of a joint in the Ithaca siltstone. Appalachian Basin, New York. In: B. Evans and T-F. Wong (Editors), Fault Mechanics and Transport Properties of Rocks. Academic Press, London, pp. 297–324.

Laubach, S.E., 1988. Subsurface fractures and their relationship to stress history in East Texas basin sandstone. Tectonophysics, 156: 37–49.

Lawn, B.R., 1993. Fracture of Brittle Solids, 2nd ed. Cambridge University Press, Cambridge, London, 378 pp.

Lawn, B.R. and Wilshaw, T.R., 1975. Fracture of Brittle Solids. Cambridge University Press, Cambridge, London, 204 pp.

Lehner, R.K., 1990. Pore-pressure-induced fracturing of petroleum source rocks: implications for primary migration. In: G. Imarisio, M. Frias and J.M. Bemtgen (Editors), Proceedings: The European Oil and Gas Conference. A.A. Balkema, Rotterdam, pp. 131–141.

Masuda, T. and Kuriyama, M., 1988. Successive 'mid-point' fracturing during microboudinage: an estimate the stress–strain relation during a natural deformation. Tectonophysics, 147: 171–177.

McClintock, F.A. and Walsh, J.B., 1963. Friction of Griffith cracks in rocks under pressure. Proc. 4th U.S. Congr. Appl. Mech., Am. Soc. Mech. Eng., pp. 1015–1021.

Mecholsky, J.J., 1994. Quantitative fractographic analysis of fracture origins in glass. In: R.C. Bradt and R.E. Tressler (Editors), Fractography of Glass. Plenum Press, New York, NY, pp. 37–76.

Meredith, P.G. and Atkinson, B.K., 1983. Stress corrosion and acoustic emission during tensile crack propagation in Whin Sill dolerite and other basic rocks. Geophys. J. R. Astron. Soc., 75: 1–21.

Michalske, T.A., 1994. Fractography of stress corrosion cracking in glass. In: R.C. Bradt and R.E. Tressler (Editors), Fractography of Glass. Plenum Press, New York, NY, pp. 111–142.

Murray, G.H., 1968. Quantitative fracture study—Sanish Pool, McKenzie Co., North Dakota. Am. Assoc. Pet. Geol. Bull., 52: 57–65.

Narr, W., 1991. Fracture density in the deep subsurface: techniques with application to Point Arguello Oil Field. Am. Assoc. Pet. Geol. Bull., 75: 1300–1323.

Nemat-Nasser S. and Horii, H., 1982. Compression-induced nonplanar crack extension with application to splitting, exfoliation and rockburst. J. Geophys. Res., 87: 6805–6821.

Nickelsen R.P., 1979. Sequence of structural stages of the Allegheny orogeny at the Bear Valley Strip Mine, Shamokin, Pennsylvania. Am. J. Sci., 279: 225–271.

Oertel, G., Engelder, T. and Evans, K., 1989. A comparison of the strain of crinoid columnals with that of their enclosing silty and shaly matrix on the Appalachian Plateau, New York. J. Struct. Geol., 11: 975–993.

Peck, L. Barton, C.C. and Gordon, R.B., 1985. Measurement of the resistance of imperfectly elastic rock to the propagation of tensile cracks. J. Geophys. Res., 90: 7827–7836.

Plumb, R.A., Engelder, T. and Yale, D., 1984a. Near surface in situ stress, 3. Correlation with microcrack fabric within the New Hampshire granites. J. Geophys. Res., 89: 9350–9364.

Plumb, R.A., Engelder, T. and Sbar, M., 1984b. Near-surface in situ stress, 2. A comparison with stress directions inferred from earthquakes, joints, and topography near Blue Mountain Lake, New York. J. Geophys. Res., 89: 9333–9349.

Pollard, D.D., 1989. Quantitative interpretation of joints and faults. Geological Society of America Short Course Notes, Annual Meeting 1989, Geol. Soc. Am., Boulder, CO, pp. 1–67.

Pollard, D.D. and Segall, P., 1987. Theoretical displacements and stresses near fractures in rock: with applications to faults, joints, veins, dikes, and solution surfaces. In: B. Atkinson (Editor), Fracture Mechanics of Rock. Academic Press, Orlando, FL, pp. 227–350.

Price, N.J., 1966. Fault and Joint Development in Brittle and Semi-brittle Rock. Pergamon Press, London, 176 pp.

Price, N.J., 1974. The development of stress systems and fracture patterns in undeformed sediments. Advances in Rock Mechanics, Proc. 3rd Congr., ISRM, I: 487–496.

Ramsay, J.G., 1980. The crack-seal mechanism of rock deformation. Nature, 284: 135–139.

Rice, J.R., 1978. Thermodynamics of the quasi-static growth of Griffith cracks. J. Mech. Phys. Solids, 26: 61–78.

Rubey, W.W., 1933. Settling velocities of gravel, sand, and silt particles. Am. J. Sci., 233: 325–338.

Rummel, R., 1987. Fracture mechanics approach to hydraulic fracturing stress measurements. In: B. Atkinson (Editor), Fracture Mechanics of Rock. Academic Press, Orlando, FL, pp. 217–240.

Secor, D.T., 1965. Role of fluid pressure in jointing. Am. J. Sci., 263: 633–646.

Secor, D.T., 1969. Mechanics of natural extension fracturing at depth in the earth's crust. In: A.J. Baer and D.K. Norris (Editors), Proc. Conf. Research in Tectonics (Kink Bands and Brittle Deformation). Geol. Surv. Can. Pap., 68-52: 3–48.

Srivastava, D. and Engelder, T., 1990. Crack-propagation sequence and pore-fluid conditions during fault-bend folding in the Appalachian Valley and Ridge. Geol. Soc. Am. Bull., 102: 116–128.

Srivastava, D. and Engelder, T., 1991. Fluid evolution history of brittle–ductile shear zones on the hanging wall of the Yellow Springs thrust, Valley and Ridge Province, Pennsylvania, U.S.A. Tectonophysics, 198: 23–34.

Steltenpohl, M.G., 1988. Kinematics of the Towaliga, Bartletts Ferry, and Goat Rock fault zones, Alabama: the late Paleozoic dextral shear system in the southernmost Appalachians. Geology, 16: 852–855.

Thiercelin, M.J. and Roegiers, J.-C., 1987. Toughness determination with the modified ring test. In: H.L., Hartman (Editor), Rock Mechanics: Key to Energy production: Proceedings of the 27th U.S. Symposium on Rock Mechanics. Society of Mining Engineers, Inc., Littleton, CO, pp. 616–622.